Electronic Supplementary Material (ESI) for Journal of Materials Chemistry A.


# Supplementary Information

## Understanding the effects of oxygen defects on the redox reaction pathways in $LiVPO_4F$ by combining *ab-initio* calculations with experiments

Heetaek Park[1], Minkyung Kim[1], ShinYoung Kang[2,*] and Byoungwoo Kang[1,*]

[1]Department of Materials Science and Engineering, Pohang University of Science and Technology (POSTECH), 77 Cheongamro, Namgu, Pohang, Gyeongbuk, Republic of Korea 790-784

[2] Lawrence Livermore National Laboratory, Livermore, California 94550, USA

* Corresponding authors

*E-mail address*: bwkang@postech.ac.kr (B. Kang)

*E-mail address*: kang10@llnl.gov (SY. Kang)

## 1. Conversion from monoclinic $VPO_4F$ to "triclinic-like" structure

The "triclinic-like" structure of monoclinic $VPO_4F$ can be obtained by following conversion steps: 1) supercell of monoclinic $VPO_4F$ was constructed, 2) triclinic-like unit cell was extracted from the supercell by setting the position of one of V ions at (0, 0, 0) as in the triclinic structures (Figure 2c), 3) lattice parameters were calculated using the positions of V ions, and 4) atomic positions of the other ions were calculated (see Figure S1, S2, and Table S1 in Supporting information).

The ground state structure of triclinic $VPO_4F$ is compared with the converted triclinic-like monoclinic $VPO_4F$ (Figures 2d and e). In the triclinic structure, there are two V sites along the c-axis direction: V1 at (0, 0, 0) and V2 at (0, 0, 0.5) where are the centers of red octahedrons in Figure 2d. While the two octahedrons are well-aligned along the c-axis direction in the monoclinic $VPO_4F$ (Figure 2e), the $VO_4F_2$ octahedrons are slightly tilted in the triclinic structure (Figure 2d), inferring that when the triclinic $Li_xVPO_4F$ ($0 \leq x \leq 1$) phase transforms to the monoclinic phase by delithiation, $VO_4F_2$ octahedrons rotate so that the tilting distortion of $VO_4F_2$ octahedrons disappears. We confirmed the propriety of our conversion process by comparing the XRD patterns of the monoclinic $VPO_4F$ before and after conversion (see Figure S3 in Supporting Information). Note that their XRD patterns are identical, and once the internal and external parameters of the triclinic-like unit cell (after conversion) are optimized, that leads to the distortion of the tilting angles of $VO_4F_2$ octahedra and the unit cell symmetry is lower to that of triclinic, $P\bar{1}$.

To compare the tavorite structure in triclinic and monoclinic phases, crystal structures of $LiVPO_4F$ (triclinic) and $VPO_4F$ (monoclinic) were investigated (Figure S1). As V1 site in triclinic structure is (0 0 0), the conversion of lattice parameters can be performed by tracing

positions of vanadium ions in monoclinic structure. It was found that [0.5 0.5 0], [0.5, -0.5 0], and [-1 0 -1] vectors in monoclinic structure correspond to [1 0 0], [0 1 0], and [0 0 1] in triclinic, respectively. By measuring lengths of these vectors and angles between them, lattice parameters can be converted from monoclinic to triclinic.

After that, the conversion matrix (*C*) was calculated to convert atomic positions from monoclinic to triclinic structure. As shown in Figure S2, calculation of each component in the 3 x 3 matrix of *C* is enabled by using lattice parameters of triclinic and monoclinic phases and the correlation between vectors in the two structures. All components of C were calculated by following these steps and then, the atomic positions of all ions (V, P, O, F) in monoclinic structure was converted to those in triclinic. To confirm whether the conversion process was successful, calculated XRD patterns of monoclinic and 'converted' triclinic $VPO_4F$ were compared (Figure S3).

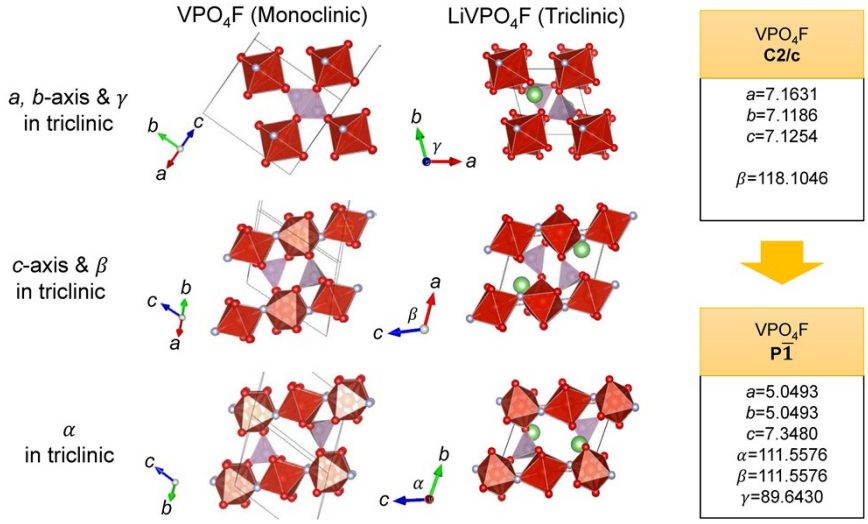


**Figure S1.** Conversion process of lattice parameters of $VPO_4F$ from monoclinic to triclinic phase by comparing $VPO_4F$ (monoclinic) and $LiVPO_4F$ (triclinic) structures: Lattice parameters of C2/c shown in the figure were obtained from Rietveld refinement of the XRD

pattern of PTFE-$VPO_4F$ based on monoclinic structure

$$\underbrace{\begin{bmatrix} a1 & a2 & a3 \\ a4 & a5 & a6 \\ a7 & a8 & a9 \end{bmatrix}}_{=C} \begin{bmatrix} 7.1631 \cdot x_{Mono} \\ 7.1186 \cdot y_{Mono} \\ 7.1254 \cdot z_{Mono} \end{bmatrix} = \begin{bmatrix} 5.0493 \cdot x_{Tri} \\ 5.0493 \cdot y_{Tri} \\ 7.3480 \cdot z_{Tri} \end{bmatrix}$$

| *Monoclinic* | *Triclinic* |
|---|---|
| [0.5 0.5 0] | [1 0 0] |
| [0.5 −0.5 0] | [0 1 0] |
| [−1 0 −1] | [0 0 1] |

**Figure S2.** Calculation of conversion matrix (*C*) using identical vectors in triclinic and monoclinic phases

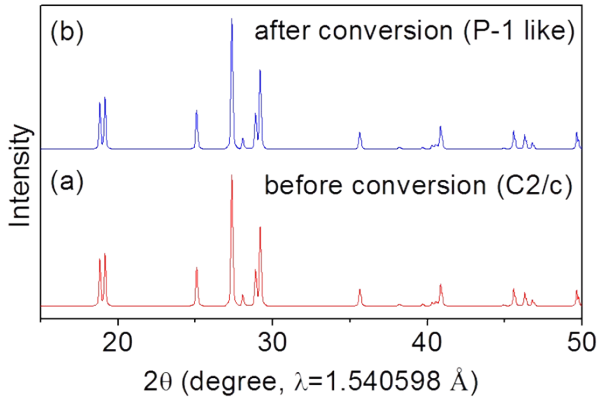


**Figure S3.** Calculated XRD pattern of (a) the original monoclinic $VPO_4F$ (C2/c), and (b) the conversed triclinic-like $VPO_4F$ ($P\bar{1}$)

## 2. Evolution of lattice parameters from NEB calculations

The lattice parameters *a*, *b*, and *c* of $VPO_4F$ (Figure S4a) and $VPO_4F_{0.917}O_{0.083}$ (Figure S4b) were also obtained. Similar to unit cell volume, *a* and *b* were irregularly changed whereas *c* continuously increased as they get closer to monoclinic (less-distorted) phase.

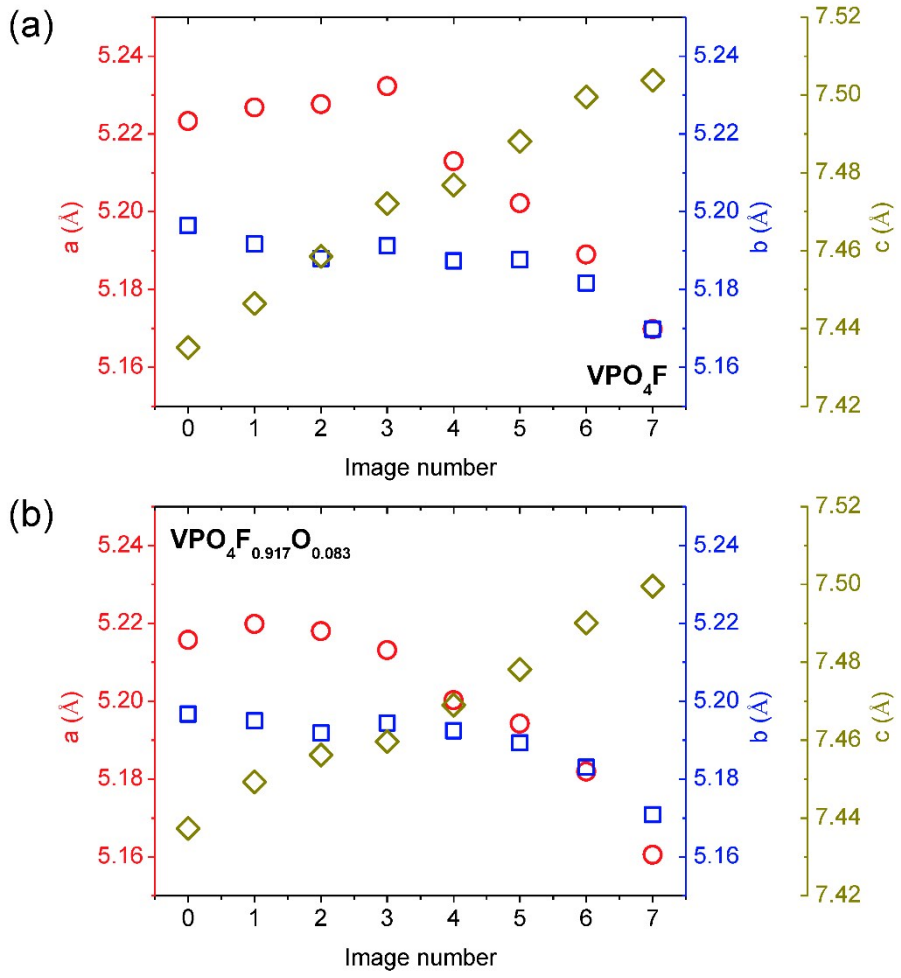


**Figure S4.** Changes in lattice parameters of (a) $VPO_4F$ and $VPO_4F_{0.917}O_{0.083}$ during phase transition obtained by NEB calculation.

## 3. Crystal structures of $LiVPO_4F$ and $VPO_4F$ obtained by PTFE and CTR processes

We use Rietveld refinement for fitting XRD data using X'pert Highscore Plus software. $LiVPO_4F$ with one Li site[1] and reported structure of $VPO_4F$[2] were used as a starting model structure. Even though we used high resolution synchrotron powder diffraction data for refining structures of the samples, it is difficult to obtain 'physically meaningful' thermal factors and occupancy, particularly for oxygen and fluorine because they have low scattering number and the data quality is not enough to refine them. Thus, we fix the thermal factors and occupancies to the known values[1, 2] (according to reference) and refined peak shape factors, lattice parameters and atom sites. We added the refined the data with fitting agreement indices in Supporting Information Table S1, S2, S3, and S4.

**Table S1. Crystal structure of PTFE $LiVPO_4F$ refined from XRD data (Figure 6a)**

| **PTFE $LiVPO_4F$ (space group: $P\bar{1}$)**<br>$a$ = 5.184 (Å), $b$ = 5.312 (Å), $c$ = 7.266 (Å), $\alpha$ = 107.58 (°), $\beta$ = 107.95 (°), $\gamma$ = 98.45 (°), V = 174.96 (Å$^3$)<br>$R_{wp}$ = 8.09, $R_{exp}$ = 3.05, $Chi^2$ = 7.04 | | | | | |
|---|---|---|---|---|---|
| atom | *x* | *y* | *z* | $B_{iso}$ | Occ. |
| V(1) | 0.0000 | 0.0000 | 0.0000 | 0.404 | 1 |
| V(2) | 0.0000 | 0.0000 | 0.5000 | 0.306 | 1 |
| P | 0.3193 | 0.6456 | 0.2514 | 0.557 | 1 |
| F | -0.1204 | 0.0925 | 0.2439 | 0.842 | 1 |
| O(1) | 0.3690 | 0.2446 | 0.5811 | 0.417 | 1 |
| O(2) | 0.1140 | 0.6696 | 0.3628 | 0.425 | 1 |
| O(3) | 0.3210 | 0.3380 | 0.1388 | 0.752 | 1 |

| | | | | | |
|---|---|---|---|---|---|
| O(4) | 0.2775 | 0.7968 | 0.0920 | 0.299 | 1 |
| Li | 0.7090 | 0.3930 | 0.2210 | 2.635 | 1 |

**Table S2. Crystal structure of CTR $LiVPO_4F$ refined from XRD data (Figure 6b)**

| **CTR $LiVPO_4F$ (space group: $P\bar{1}$)** | | | | | |
|---|---|---|---|---|---|
| $a$ = 5.176 (Å), $b$ = 5.308 (Å), $c$ = 7.265 (Å), $\alpha$ = 107.58 (°), $\beta$ = 107.98 (°), $\gamma$ = 98.36 (°), V = 174.62 (Å$^3$) | | | | | |
| $R_{wp}$ = 7.10, $R_{exp}$ = 2.82, $Chi^2$ = 6.34 | | | | | |
| atom | *x* | *y* | *z* | $B_{iso}$ | Occ. |
| V(1) | 0.0000 | 0.0000 | 0.0000 | 0.404 | 1 |
| V(2) | 0.0000 | 0.0000 | 0.5000 | 0.306 | 1 |
| P | 0.3184 | 0.6470 | 0.2511 | 0.557 | 1 |
| F | -0.1154 | 0.0903 | 0.2491 | 0.842 | 1 |
| O(1) | 0.3707 | 0.2373 | 0.5744 | 0.417 | 1 |
| O(2) | 0.1103 | -0.3280 | 0.3702 | 0.425 | 1 |
| O(3) | 0.6898 | 0.6659 | -0.1371 | 0.752 | 1 |
| O(4) | 0.2766 | 0.7885 | 0.0889 | 0.299 | 1 |
| Li | 0.7040 | 0.3900 | 0.2000 | 2.635 | 1 |

**Table S3. Crystal structure of PTFE $VPO_4F$ refined from XRD data (Figure 7b)**

| **PTFE $VPO_4F$ (space group: $P\bar{1}$)** | | | | | |
|---|---|---|---|---|---|
| $a$ = 5.048 (Å), $b$ = 5.053 (Å), $c$ = 7.351 (Å), $\alpha$ = 111.54 (°), $\beta$ = 111.59 (°), $\gamma$ = 89.64 (°), V = 160.39 (Å$^3$) | | | | | |
| $R_{wp}$ = 12.57, $R_{exp}$ = 4.42, $Chi^2$ = 8.08 | | | | | |
| atom | x | y | z | $B_{iso}$ | Occ. |
| V(1) | 0.0000 | 0.0000 | 0.0000 | 0.971 | 1 |
| V(2) | 0.0000 | 0.0000 | 0.5000 | 1.489 | 1 |
| P | 0.3975 | 0.6422 | 0.2442 | 0.241 | 1 |
| F | -0.0699 | 0.1024 | 0.2321 | 4.080 | 1 |

| | | | | | |
|---|---|---|---|---|---|
| O(1) | 0.2977 | 0.3023 | 0.6568 | 0.455 | 1 |
| O(2) | 0.2622 | -0.2277 | 0.4225 | 0.455 | 1 |
| O(3) | 0.3158 | 0.3085 | 0.1520 | 0.455 | 1 |
| O(4) | 0.2308 | 0.7360 | 0.0861 | 0.455 | 1 |

**Table S4. Crystal structure of CTR $VPO_4F$ refined from XRD data (Figure 7a)**

| **CTR $VPO_4F$ (space group: $P\bar{1}$)**<br>$a$ = 5.056 (Å), $b$ = 5.051 (Å), $c$ = 7.355 (Å), $\alpha$ = 111.57 (°), $\beta$ = 111.48 (°), $\gamma$ = 89.70 (°), V = 160.73 (Å$^3$)<br>$R_{wp}$ = 9.60, $R_{exp}$ = 4.46, $Chi^2$ = 4.63 | | | | | |
|---|---|---|---|---|---|
| | *x* | *y* | *z* | $B_{iso}$ | Occ. |
| V(1) | 0.0000 | 0.0000 | 0.0000 | 0.672 | 1 |
| V(2) | 0.0000 | 0.0000 | 0.5000 | 1.191 | 1 |
| P | 0.3638 | 0.6188 | 0.2503 | 0.629 | 1 |
| F | 0.9021 | 0.0706 | 0.2643 | 0.941 | 1 |
| O(1) | 0.2969 | 0.3067 | 0.6539 | 0.062 | 1 |
| O(2) | 0.2435 | 0.7555 | 0.4141 | 0.062 | 1 |
| O(3) | 0.3117 | 0.2970 | 0.1552 | 0.062 | 1 |
| O(4) | 0.2408 | 0.7406 | 0.0740 | 0.062 | 1 |

## References


1. J.-M. Ateba Mba, C. Masquelier, E. Suard and L. Croguennec, *Chemistry of Materials*, 2012, **24**, 1223-1234.

2. B. L. Ellis, T. N. Ramesh, L. J. M. Davis, G. R. Goward and L. F. Nazar, *Chemistry of Materials*, 2011, **23**, 5138-5148.